**Advances in Concrete Construction**, *Vol. 3, No. 2 (2015) 127-143*
DOI: http://dx.doi.org/10.12989/acc.2015.3.2.127 

# Numerical modelling of the pull-out response of inclined hooked steel fibres

Kyriaki Georgiadi-Stefanidi[a], Olympia Panagouli[*] and Alexandra Kapatsina[b]

*Laboratory of Structural Analysis and Design, Department of Civil Engineering, University of Thessaly, Pedion Areos, 38334 Volos, Greece*

*(Received March 16, 2015, Revised June 25, 2015, Accepted July 10, 2015)*

**Abstract.** Steel fibre reinforced concrete (SFRC) is an anisotropic material due to the random orientation of the fibres within the cement matrix. Fibres under different inclination angles provide different strength contribution of a given crack width. For that the pull-out response of inclined fibres is of great importance to understand SFRC behaviour, particularly in the case of fibres with hooked ends, which are the most widely used. The paper focuses on the numerical modelling of the pull-out response of this kind of fibres from high-strength cementitious matrix in order to study the effects of different inclination angles of the fibres to the load-displacement pull-out curves. The pull-out of the fibres is studied by means of accurate three-dimensional finite element models, which take into account the nonlinearities that are present in the physical model, such as the nonlinear bonding between the fibre and the matrix in the early stages of the loading, the unilateral contact between the fibre and the matrix, the friction at the contact areas, the plastification of the steel fibre and the plastification and cracking of the cementitious matrix. The bonding properties of the fibre-matrix interface considered in the numerical model are based on experimental results of pull-out tests on straight fibres.

**Keywords:** hooked steel fibres; inclination angle; pull-out strength; high-strength cementitious matrix; three-dimensional finite element modelling

## 1. Introduction

The last four decades research studies on fibre reinforced concrete have proved that the addition of steel fibres in concrete or in most kinds of cementitious mixtures, can improve significantly their tensile strength. The beneficial effect of the fibres becomes obvious after matrix cracking has occurred, as they tend to restrict the growth of cracks and undertake the tensile forces immediately after the exhaustion of the tensile strength of the matrix. As each crack continues to open, the fibres that are "bridging" the crack are being pulled-out from the cementitious matrix. Thus, it can be said that the post-cracking behaviour of a steel-fibre reinforced cementitious matrix

[*] Corresponding author, Assistant professor, E-mail: olpanag@uth.gr
[a] Dr., E-mail : kelly.geo@gmail.com
[b] Msc., E-mail : alexandra@sdeng.gr


http://www.techno-press.org/?journal=acc&subpage=7 ISSN: 2287-5301 (Print) 2287-531X (Online)

(SFRCM) is influenced by the effectiveness of the steel fibres in the mixture. The effectiveness of a single fibre can be determined through the load – slip curve which is obtained by the pull-out test of the fibre.

The first steel fibres that were used for the production of fibre reinforced concretes were straight ones. A lot of analytical models were developed for the explanation of their beneficial effect in the overall performance of the mixture. The overall behaviour of a straight steel fibre during a pull-out test is characterized by the bond between the fibre and the matrix and for that several researchers attempted to investigate experimentally, numerically or analytically the properties of the fibre-matrix interface (Mobasher and Li 1995, Shannag *et al.* 1996, Li and Mobasher 1998, Tsai *et al.* 2005).

Later, steel fibres of improved shape were introduced, such as hemi-circular, curved, waved and hooked ones. It was demonstrated by various researchers that the use of these steel fibres of improved shape leads to better performance with respect to straight ones in terms of compressive concrete strength (Ezeldin and Lowe 1991), flexural strength (Ramakrishnan *et al.* 1989, Ezeldin and Lowe 1991, Balaguru *et al.* 1992, Zhan *et al.* 2014), shrinkage (Pailleve *et al.* 1989), etc. Generally, in the case of hooked fibres researchers focus on the strengthening contribution provided by the hook on the pull-out response (Alwan *et al.* 1999, Sujivorakul *et al.* 2000, Kangaj *et al.* 2014).

Considering a specific type of steel fibres and for a given volumetric ratio of these fibres in the mixture, the post-cracking properties of the SFRCM are influenced by the random distribution and random orientation of the fibres in the mixture. Several researchers have tried to investigate either experimentally or analytically the pull-out behaviour of inclined steel fibres. For example, Chanvillard and Aitcint (1996) performed several pull-out tests of corrugated steel fibres, investigating the effect of the fibre length, its orientation with respect to the cracked plane ($45^o$ and $90^o$ angle) and the water to cement ratio of the matrix. Robins *et al.* (2002) investigated the effects of matrix strength, fibre embedment length and orientation, in the pull-out response of hooked-end steel fibres. Banthia and Trottier (1994) experimentally investigated the bond-slip characteristics for three types of deformed steel fibres in concrete matrices with different strengths, which were aligned at 0, 15, 30, 45 and 60 degrees with respect to the loading direction. They also correlated the results obtained from the pull-out tests to the actual behaviour of the fibre reinforced concrete. Finally, Lee *et al.* (2010), Laranjeira *et al.* (2010a), Laranjeira *et al.* (2010b), Soetens *et al.* (2013) and Zhan and Meschke (2014) have proposed analytical methods to predict the pull-out response of inclined straight or hooked steel fibres in an ultra-high strength cementitious matrix.

The present work focuses on hooked-end steel fibres in a high-strength cementitious matrix. In order to investigate the pull-out response of these fibres, detailed three-dimensional models were realized using the Finite Element (F.E.) method. Three cases are studied corresponding to different orientation angles of the fibres with respect to the cracked plane of the cementitious matrix, namely $15^o$, $30^o$ and $45^o$. The results obtained from each numerical model are compared to the experimental and numerical results obtained from the pull-out of an aligned fibre (Georgiadi-Stefanidi *et al.* 2010a), in order to study the effect of the fibre orientation angle in the pull-out load-displacement curves.

## 2. Pull-out behaviour of inclined hooked fibre

The pull-out behaviour of inclined hooked fibres includes all the phenomena that the pull-out

behaviour of inclined straight fibres presents such as fibre debonding, matrix spalling, frictional sliding and fibre removal. Moreover, hooked ends imply plastic deformations which increase the force required to pull-out the fibre, and so magnifying the matrix spalling effects of inclined fibres.

From the research of Pompo *et al.* (1996), it results that a typical pull-out response of inclined fibres consists of four distinct regions

- elastic response followed by debonding;
- fibre pull-out and strengthening process;
- frictional sliding within the straight matrix duct;
- fibre removal from the matrix.

### *2.1 Experimental observations*

Tests on inclined fibres showed that crack widths at peak increase with the inclination angles (Armelin and Banthia 1997, Robins *et al*. 2002) and it was found that this increase was generally independent of fibre embedded length providing that the hook end was fully mobilized. These increments of crack width have their nature to the combination of fibre strengthening with crushing and spalling of the concrete that takes place at the corner where fibre exits the matrix (Bartos and Duris 1994). It was also observed that at large inclination angles the pull-out response becomes progressively less influenced by the matrix strength and is governed by the mechanical properties of the fibre as it attemps to straighten in line with the loading direction.

It has been observed that optimum peak loads of hooked fibres occur in cases where inclinations angles are within $10^{o}$-$30^{o}$. In these cases experimental results showed that the increasing at peak load is up to 20% compared to aligned fibres. These observations change when fibre rupture occurs, fact which leads to a brittle failure model.

The same experimental works showed that the load at which fibres fail decreases as inclination angle increases. The reduction of the ultimate load was explained by Bartos and Duris 1994 who introduced a new fibre characteristic, the "inclined tensile strength" which takes into account bending and shear stresses that exist at the fibre exit point.

It has also been observed that for fibres under large inclination angles the axial component of the pull-out mechanism is not dominant and rupture tends to occur due to attainment of the ultimate strain capacity of the steel at the exit point from the matrix. Although this is the most common location where rupture occurs (Cunha *et al.* 2007) fracture at the hook portion has also been observed (Robins *et al.* 2002). This has its nature to the fact that the distance between the fibre exit point and the portion where the hook is located is small, typically in cases when matrix spalling produces small fibre embedded lengths. In these cases bending stresses generated by local curvature extend towards inner sections of the fibre, and hence rupture at the hook portion occurs as result of bending stresses in conjunction with the stresses resulting from the straightening process.

### *2.2 Interpretation of the pull-out response*

Taking into account the experimental results reported in literature, eight key-points may be identified on the experimental pull-out diagrams of inclined steel fibres with hooked ends. According to Laranjeira *et al.* (2010b), the initial branch of the pull-out process is similar to the one denoted by inclined straight fibres. As it is shown in Fig. 1 (point $H_1$) the pull-out response

enters into an unstable phase in which bending of the debonded segments of the fibre tends to impose failure of the matrix at the crack surface when fibre debonding occurs. The larger the inclination angle, the larger are the matrix spalling effects and the smaller is the contribution provided by the hook at point $H_2$. When the maximum contribution provided by the hook is attained (point $H_3$) no further spalling occurs and pull-out develops under a more stable mechanism. The post-peak branch is then characterized by three key-points ($H_4, H_5, H_6$) whose relative slippages are associated to the geometry of the hook.

When the end of the hook of the fibre enters the initial straight segment of the duct (point $H_6$) no further plastic deformation occur. Then friction becomes the most dominant mechanism and the load carrying capacity decreases proportionally to the available embedded length at an almost constant rate. When the remaining embedded length tends to zero the pull-out load depends mainly on the deviation force at fibre exit point. Thus when a critical embedded length is reached (point $H_7$) the load sharply decreases to zero (point $H_8$).

## 3. Pull-out model

The composite material studied here consists of a high-strength cementitious matrix with the addition of hooked-end steel fibres. The cementitious matrix has a compressive strength of 100 MPa and a tensile strength of 8 MPa. The stainless steel fibres used in this mixture have circular shape, diameter *d*=0.4 mm and the mean dimensions are given in Fig. 2 (in mm). The chemical composition of the fibres is similar to the grade SS310 stainless steel, which has a very high ultimate elongation strain. Due to the fact that they are cold-drawn, they exhibit a nominal yield stress of 1400 MPa.

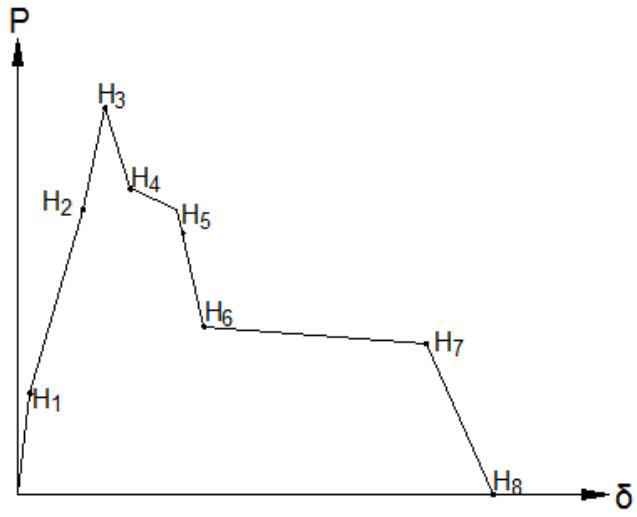


Fig. 1 Schematic diagram of the pull-out model for inclined fibres with hooked ends

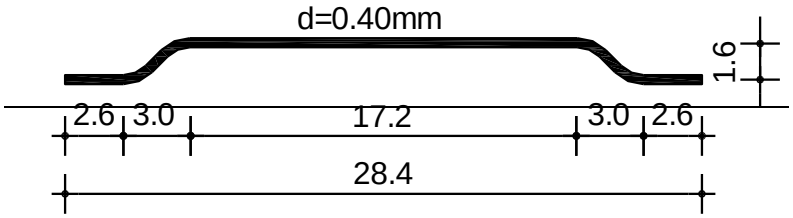


Fig. 2 Dimensions of the steel fibres used

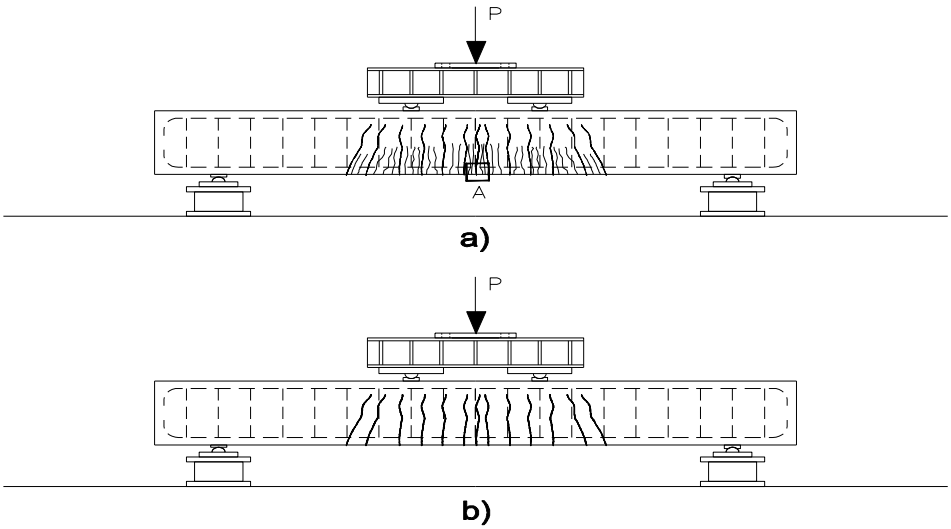


Fig. 3 Comparison of the performance between two types of beams: (a) fibre reinforced concrete beam with longitudinal and transverse reinforcement and (b) standard reinforced concrete beam

The composite material can be used for the construction of new structural members (beams, columns, etc), but it can be also used effectively for the strengthening of existing reinforced concrete elements in the form of thin jackets (Georgiadi-Stefanidi *et al.* 2010b). Its excellent rheological properties make possible the filling of very tight formworks. All these members receive, in addition to the steel fibres, ordinary longitudinal and transverse reinforcement. In the case of a SFRCM beam with ordinary reinforcement, subjected to four-point bending (Fig. 3(a)), a rather ductile behaviour is observed. Compared to a conventional reinforced concrete beam (Fig. 3(b)), the SFRCM beam exhibits very narrow and closely spaced cracks, few of which develop in width as the load approximates the maximum loading that the beam is able to undertake. Fig. 4 shows area "A" of Fig. 3(a), magnified several times. Actually, it represents the lower edge of the SFRCM beam, where tensile stresses appear. After the exhaustion of the tensile strength of the matrix, the first cracks start to occur. At that point, stress redistribution starts, as the forces previously undertaken by the tensile strength of the cementitious matrix, have to be transferred to the steel fibres. As soon as a single fibre starts to fail, the forces that it undertakes are transferred to the neighbouring fibres as well as to the longitudinal reinforcement.

Although the fibres are randomly distributed in the mixture and have also a random orientation, it has been noticed that directivity effect occurs close to the edges of the structural members. This effect together with the effect of vibration, especially in mixtures with increased workability, leads

to steel fibres oriented almost horizontally near the lower mould of the structural members (Dupont and Vanderwalle 2005). Of course, this directivity effect eliminates the randomness only with respect to 1 of the 3 spatial directions. The fibres are left oriented randomly with respect to a plane which is parallel to the corresponding face of the structural member. The pull-out behaviour of the fibres that are oriented perpendicularly or almost perpendicularly to the formed crack is dominated by the debonding of the fibre-matrix interface, the friction mechanism and the plastification of the hook due to bending, during the slip of the fibre (Fig. 5(a)). However, the fibres which are not oriented perpendicularly or almost perpendicularly to the formed crack, as it has been already mentioned, exhibit a more complex behaviour due to additional friction mechanisms, the bending of the fibres at the crack surface and the spalling of the matrix (Fig. 5(b)).

Therefore, fibres with different inclination angles with respect to the cracking plane and for a given crack width can result to different maximum strength values. This paper focuses on the numerical modelling of the pull-out of inclined hooked steel fibres from high-strength cementitious matrix. The numerical analysis of the problem presents a number of numerical difficulties requiring special treatment. During the pull-out process, the following nonlinear phenomena evolve and interact with each other:

- the nonlinear bonding between the fibre and the matrix in the early stages of the loading;
- the unilateral contact between the fibre and the matrix;
- the friction at the areas of the fibre and the matrix which come in contact;
- the plastification of the steel fibre;
- the plastification or even crushing of the cementitious matrix in compression regions and the cracking in regions where tensile stresses appear;
- the occurrence of large displacements and large strains during the movement of the steel fibre;
- the spalling of the matrix at the exit point of the fibre.

The effect of different inclination angles of the fibres to the load-displacement pull-out curves are studied through the comparison of the numerical results with the $P$-$\delta$ curve obtained from the pull-out of an aligned fibre from the cementitious matrix (Georgiadi-Stefanidi *et al.* 2010a).

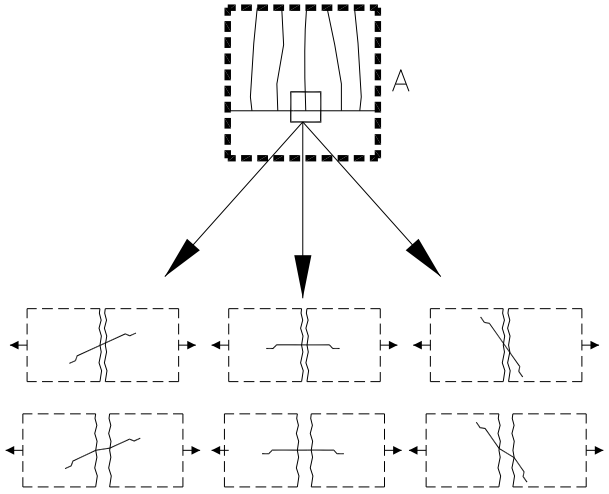


Fig. 4 Magnification of the area designated with “A” in Fig. 3

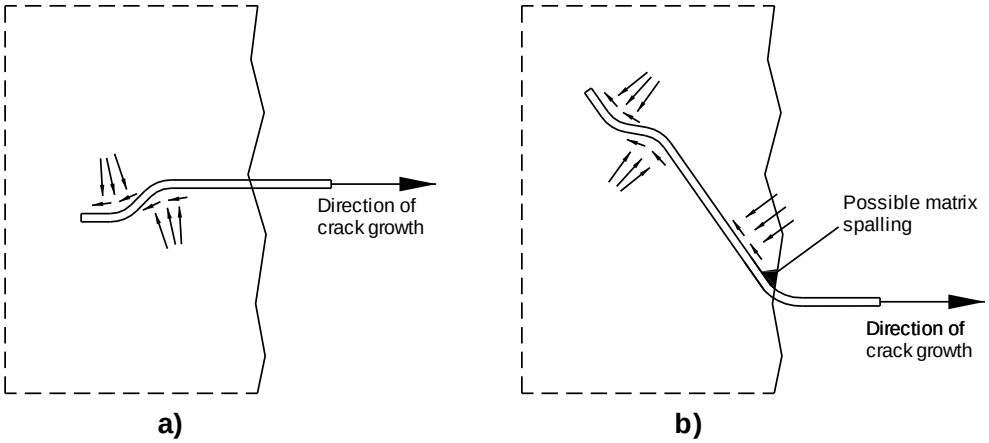


Fig. 5 Fibre pull-out: (a) with the simplest friction mechanism (friction forces in the vicinity of the two bended parts of the fibre) and (b) with multiple friction mechanisms

## 4. The principles of numerical simulation

### *4.1 Geometry of the problem*

The geometry of the various models studied here is shown in Fig. 6. The symmetries that exist in the physical model were utilized in order to limit the size of the numerical problem. Therefore, only half of the original model was considered (using the appropriate boundary conditions), in which a part of the stainless steel fibre is embedded in the cementitious matrix. For the later, a cylindrical volume was considered, with diameter large enough so that it can be assumed that the value of this diameter does not influence the results of the analysis. Here, this diameter was taken equal to 7.6 mm. It should be noticed that the geometry of the matrix indicates the direction of the considered crack plane, for every case. For the case where the fibre is oriented perpendicularly to the formed crack, the pull-out load is applied axially on the fibre. On the other hand, for the case of the inclined fibres, the pull-out load is applied on the fibre with a direction perpendicular to each crack face, that is, with the corresponding inclination angle with respect to the axis of the fibre.

### *4.2 The finite element model*

Due to the specific geometry and the existence of the various already mentioned nonlinearities, three-dimensional modelling is used. Both the cementitious matrix and the steel fibre were simulated by 10-node tetrahedral finite elements, as shown in Fig. 7. The much denser discretization of the fibre is necessary in order to simulate accurately the bending behaviour that dominates the pull-out process, as well as to reproduce in detail the elaborate geometry of the fibre. Moreover, for the models simulating the pull-out of the inclined fibres, the F.E. mesh of the matrix near the exit point of the fibre is denser with respect to the rest of the volume of the matrix, in order to simulate more accurately the possible spalling of the matrix and also, to help the optimization of the stability of the numerical algorithm.

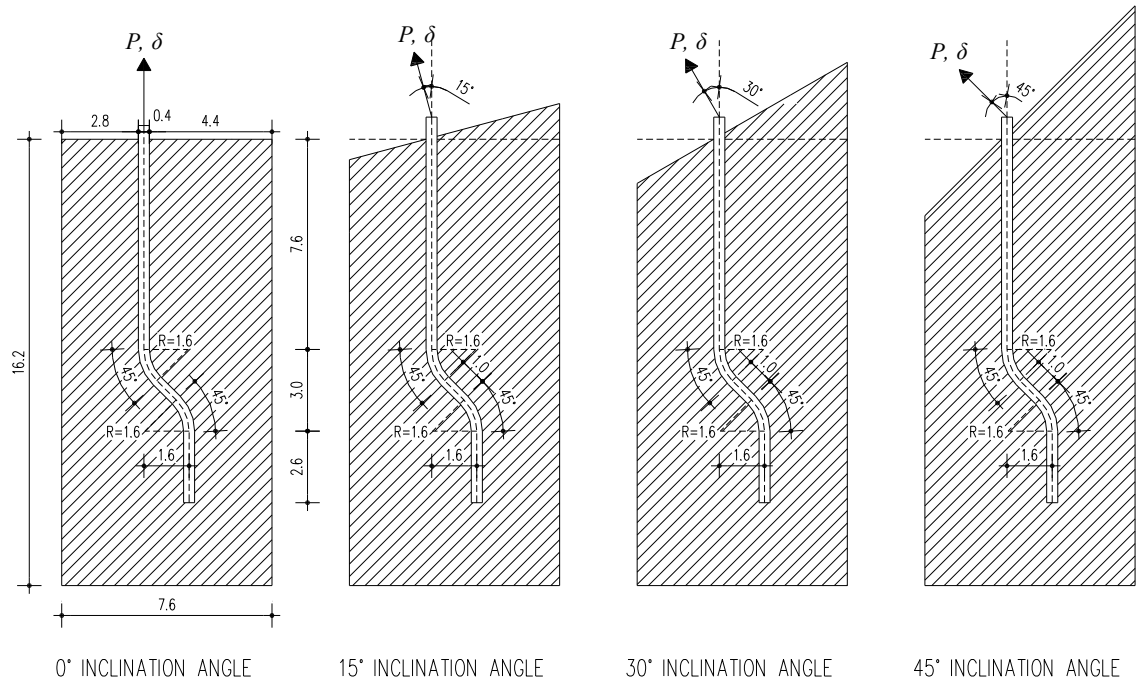


Fig. 6 The considered problem of the pull-out of inclined fibres

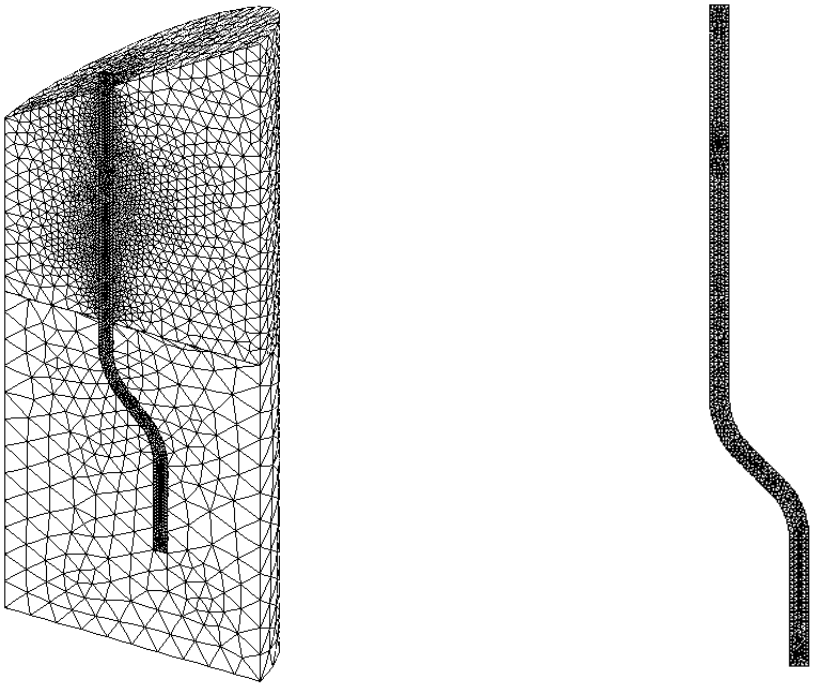

Fig. 7 The three-dimensional F.E. mesh for the case of fibre with $30^o$ inclination angle and detail of the F.E. mesh of the steel fibre

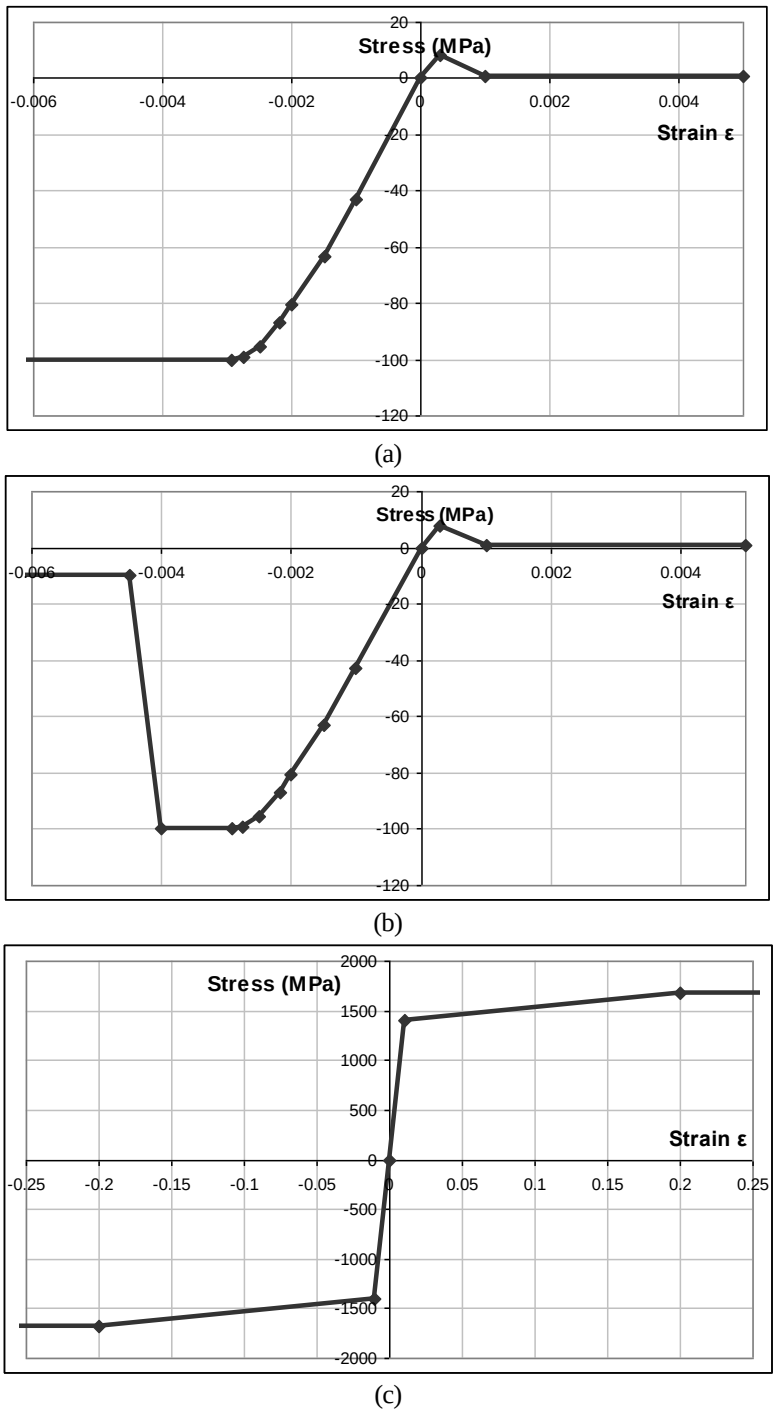


Fig. 8 The considered stress-strain relationships for: (a) the confined cementitious matrix, (b) the unconfined cementitious matrix and (c) the steel fibres

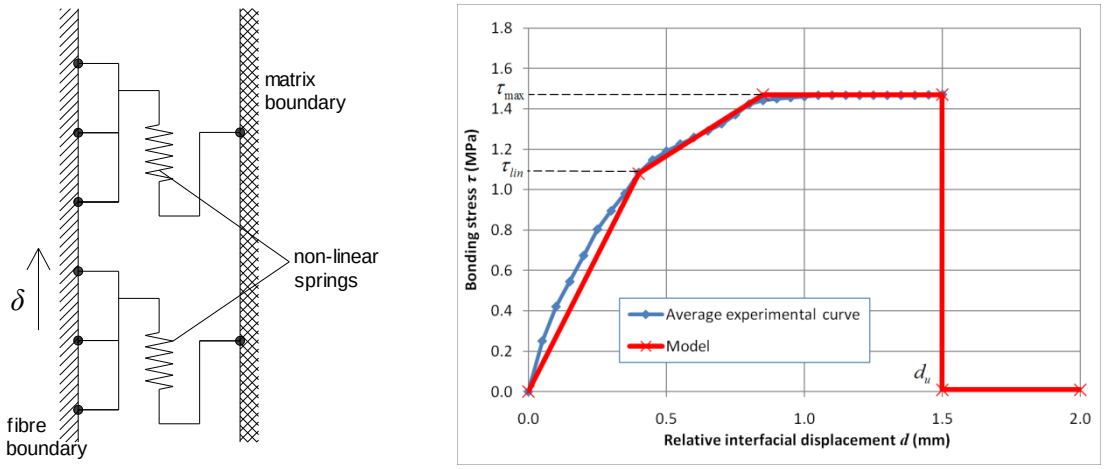


Fig. 9 Schematic presentation of the function of the interfacial elements between the steel fibre and the cementitious matrix and the piecewise linear law adopted for the interfacial elements

### *4.3 Material properties*

The compressive strength of the cementitious matrix is 100 MPa, while the tensile strength is 8 MPa. The stress-strain relationship assumed for the matrix exhibits elastoplastic behaviour for compression and a cracking behaviour in tension. The loss of the tensile strength after cracking is modelled through a softening branch having a slope $k_s$=$10^7$ MPa. As far as the behaviour of the matrix in compression is concerned, two different cases are considered, according to the confinement conditions. In the lower half of the matrix, the plastification or cracking in the matrix is limited in an area very close to the fibre, mainly due to the interaction between the matrix and the fibre during the pull-out. This region is considered to be confined by the rest of the volume of the cementitious matrix and the stress-strain relationship of Fig. 8(a) is assumed to hold. On the other hand, in the upper half of the matrix, damage occurs mainly in the area of the exit point of the fibre, where possible spalling of the matrix can occur. This region is considered as unconfined and the stress-strain relationship of Fig. 8(b) is assumed to hold. The compressive strength of the matrix is almost zeroed for a strain larger than 0.005 (Papanikolaou and Kappos 2007). The elasticity modulus of the matrix is 29 GPa and the Poisson's ratio is taken equal to 0.2. The elasticity modulus of the stainless steel fibre is taken equal to 210 GPa and the Poisson's ratio equal to 0.3. The stress-strain relationship that is used for the fibre is depicted in Fig. 8(c).

### *4.4 Bonding and friction mechanisms*

During a pull-out test, the load is being transferred through the fibre-matrix interface, first by the bond shear stresses and afterwards by the frictional stresses. Therefore, two different mechanisms must be taken into account.

Here the bonding mechanism was taken into account by introducing interfacial elements. These elements are actually nonlinear springs, acting only in the tangential to the interface direction, which are equipped with a nonlinear law. The first node of the springs is connected to the fibre. Due to the fact that the discretization densities are not similar for the firbre and for the matrix, the

second node of the spring is attached to the closest matrix node, as shown in Fig. (9). The nonlinear behaviour of these elements was estimated after the pull-out tests of straight fibres from the cementitious matrix (Georgiadi-Stefanidi *et al.* 2010a), as in the case of straight fibres the bond between the two materials is dominant. Fig. (9) gives also, the average experimental pull-out curve obtained by these tests. The horizontal axis of the diagram gives the relative interface displacements, while the vertical axis gives the value of the developed bonding stress. This experimental diagram was approximated by a piecewise linear curve defined by the characteristic values $\tau_{lin}$, $\tau_{\max}$ and $d_u$. The pull-out behaviour is more or less linear until the bonding stress reaches the value $\tau_{lin}$. After this value, a significant stiffness reduction is observed, until the value $\tau_{\max}$ is achieved. For a certain displacement range this value remains constant and after a characteristic displacement value $d_u$ is achieved, the resistance is zeroed. The interfacial elements were assumed to follow this piecewise linear law.

The second mechanism that had to be simulated was the friction one. The pull-out behaviour of a hooked-end fibre is dominated by the mechanical interlock and the plastification of the hooked end. Because of this mechanical interlock, normal forces develop on the fibre-matrix interface during the pull-out process, resulting to the appearance of the primary friction mechanism in the contact areas. The contact and friction forces were taken into account by introducing unilateral contact and friction conditions between the fibre-matrix interface. For the friction, a simplified Coulomb model was taken into account. The friction coefficient was taken equal to 0.1, after the comparison of the results obtained from the numerical simulation of the pull-out of an aligned hooked fibre and the corresponding experimental results (Georgiadi-Stefanidi *et al.* 2010a). A numerical parametric analysis was performed, considering different values for the friction coefficient in the range between $\mu$=0 and $\mu$=0.2. After the comparison of the *P-δ* diagrams that resulted from the parametric analysis with the average experimental curve, it was concluded that the average strength value of the experimental results is well approximated by a friction coefficient of the order of $\mu$=0.1.

### *4.5 Solution control*

The solution to the above problem was obtained by using the software code MSC-MARC. A von Mises plasticity criterion was used together with an isotropic hardening rule for the expansion of the yield surface. As the problem involves significant geometry changes during the solution process, the Updated Lagrange large displacement procedure was preferred, in order to improve the convergence speed. Moreover, a large strain formulation was applied in order to handle correctly the large strains that appear during the pull-out process. Finally, a double-sided contact procedure was used, in order to avoid penetrations of the one contact body into the other. A Newton-Raphson iterative procedure was applied in order to handle the nonlinearities of the problem. The load was applied in the form of displacement, at the top end of the steel fibre. The resulting force at the point of the applied displacement was monitored. It was decided to apply a modified version of the standard Newton-Raphson procedure, in which the stiffness matrix was reassembled in every iteration. This procedure, although it seems to be more costly from the computational point of view, finally it proved to be very efficient due to the high nonlinear nature of the problem. A relative convergence criterion was adopted, based on the residual forces and the relative force tolerance was set 0.01.

## 5. Results and discussion

The results obtained by the numerical models simulating the pull-out test of an aligned fibre and of inclined fibres with inclination angles of 15°, 30° and 45°, are presented in this section. In Fig. 10, the *P-δ* curves obtained by the aforementioned 3D numerical models are compared. In general, until a displacement of 0.15 mm, the behaviour of the problem is almost linear. After this point, the steel fibre begins to yield and plastic hinges are formed in different locations of the bended part of the fibre, as it tends to change shape and be pulled-out of the matrix (see Fig. 11). This process results in the significant decrease of the slope of the *P-δ* diagrams after a displacement of about 0.15 mm. Moreover, the matrix in the vicinity of the bended parts of the fibre is stressed and plastified due to the interaction between the fibre and the matrix. Fig. 12 presents the plastic strain fields in the matrix in this vicinity for displacements of 0.5 mm and 1.0 mm obtained by the numerical models of the aligned fibre and all the cases of the inclined fibres studied. It is noticed that these plastic strain fields are very similar for the aligned and for all the inclined fibres, in terms of shape, position and strain values.

After the displacement of 1.5 mm, the bonding strength is exhausted and this corresponds to the abrupt decrease of the resistance, which is noticed in the *P-δ* curves. After this decrease, however, the force increases again, due to the friction which becomes the dominant mechanism. Finally, the decrease of the pull-out force starts after a displacement of about 2.8 mm, when the fibre starts to lose its doubly bended shape, as it is being pulled-out from the matrix and the main resistance to the pull-out is the friction and contact mechanism (Georgiadi-Stefanidi *et al*. 2010a).

However, besides the above described process, the behaviour of the fibres that are pulled-out from the cementitious matrix with an inclination angle is influenced by additional mechanisms such as the bending of the fibre near the exit point in conjunction with the additional friction forces developed there and the crushing of the matrix near the same area. Due to this fact, the maximum value of the pull-out load differs for each inclination angle. It is important to mention here that in the case of fibres under large inclination angles, local friction at the fibre exit point and crushing of the matrix near this area govern the pull-out process, thus postponing the anchoring effects provided by the hook.

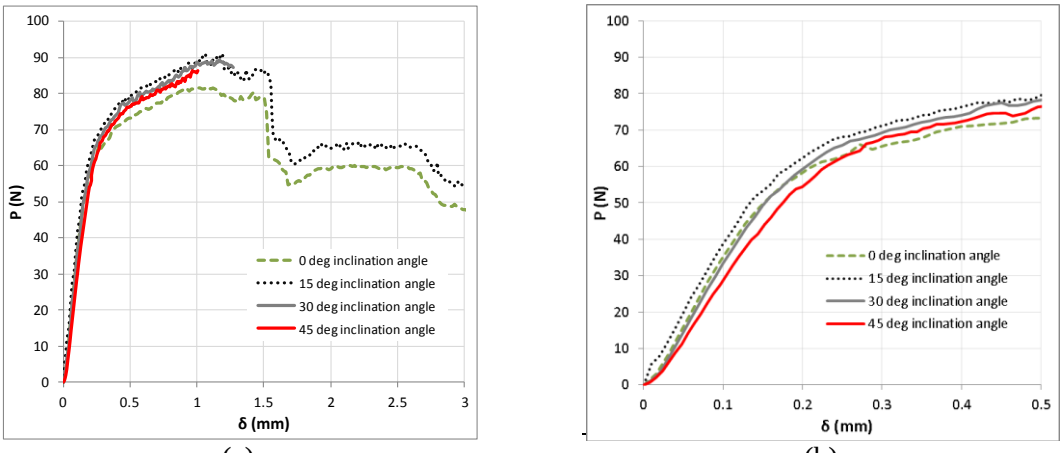


Fig. 10 (a) Comparison of the *P-δ* diagrams obtained by the 3D model for various values of the inclination angle of the fibre, (b) detail of previous diagram for small values of the displacement

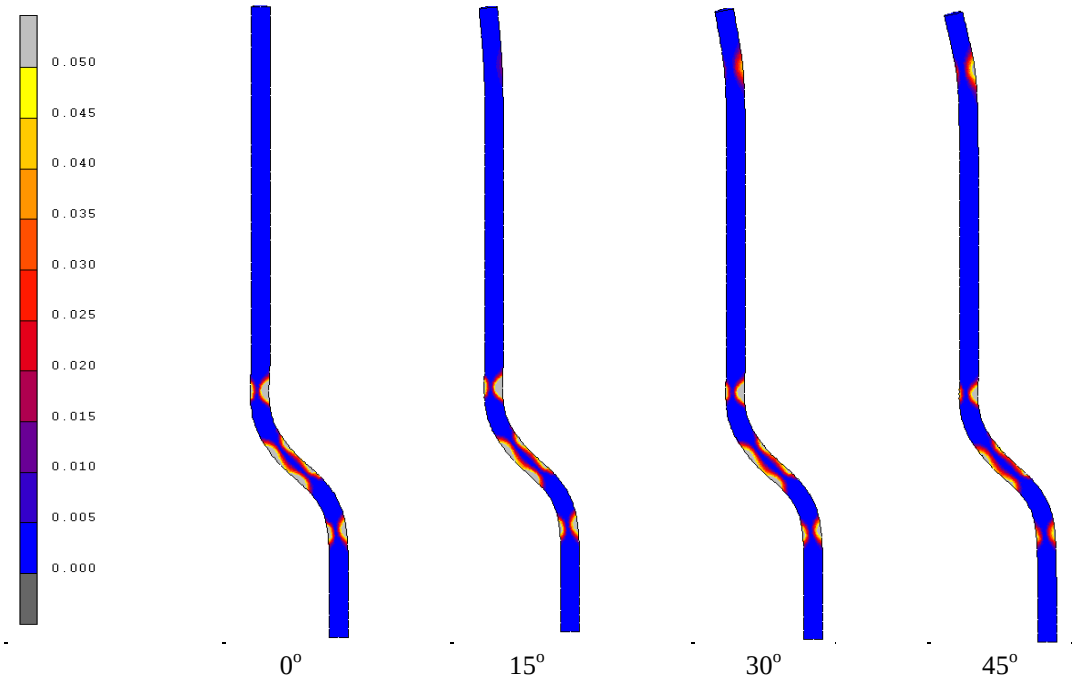


(a)

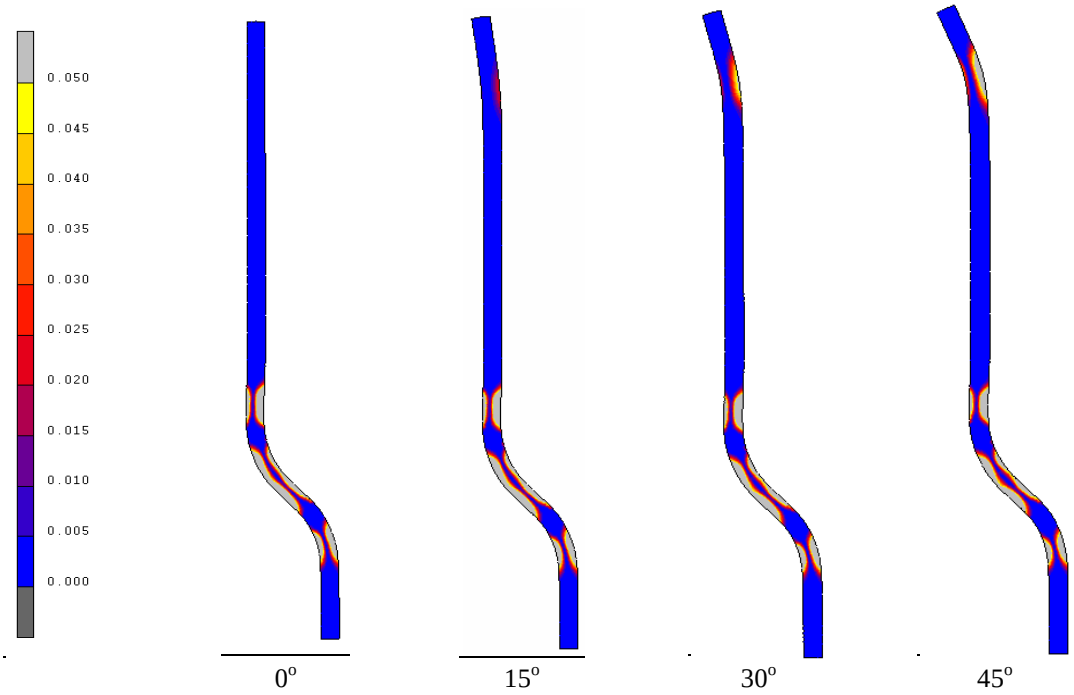


(b)

Fig. 11 Plastic strain fields of the steel fibres for a displacement (a) $\delta$=0.5 mm and (b) $\delta$=1.0 mm

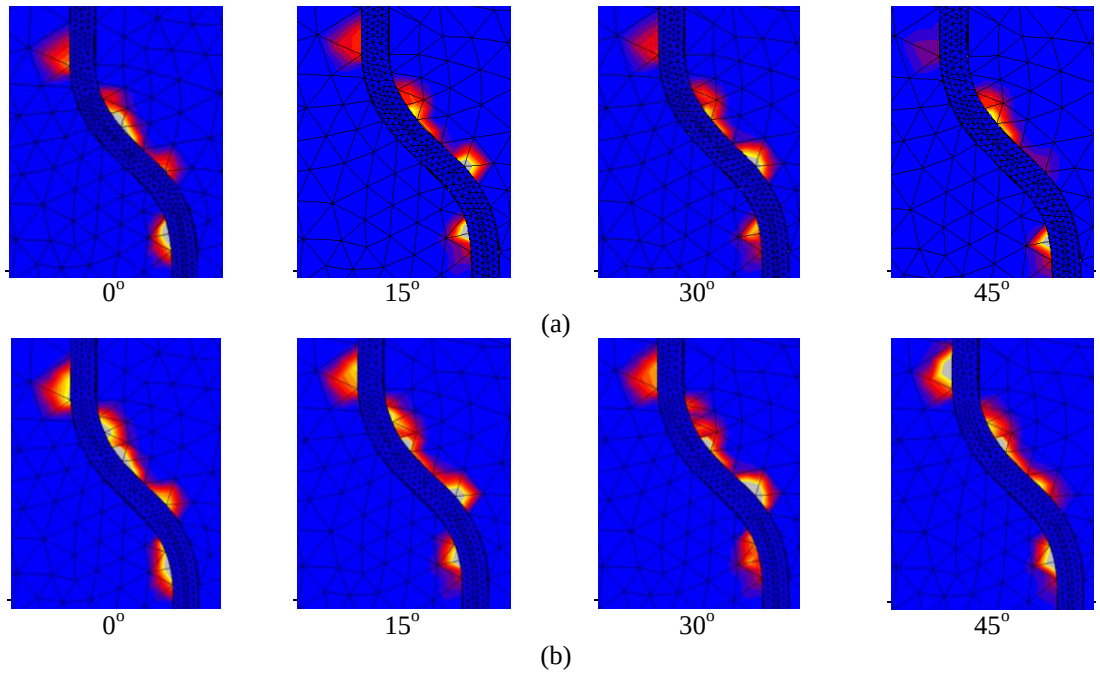


Fig. 12 Plastic strain fields of the cementitious matrix for a displacement (a) $\delta$=0.5 mm and (b) $\delta$=1.0 mm

Fig. 11 presents the plastic strain fields of the fibres that arise during the pull-out, for displacements of 0.5 mm and 1.0 mm. It is noticed that the plastic hinges that are formed in the neighbourhood of the hooked end of the fibre are common for all the studied cases. The difference between the aligned and all the inclined fibres lies in the fact that additional plastic deformations appear in the inclined fibres at their upper part, near their exit point from the matrix, due to bending. Moreover, as it is clearly shown in Fig. 11, as the inclination angle increases, the corresponding plastic deformation becomes greater. This fact could lead to the assumption that for the fibres that present greater deformations due to bending, the maximum pull-out strength value will be larger. However, this assumption is contradicted by the results obtained by the numerical models, which were given in Fig. 10. This is due to the fact that as it has been already observed (Cunha *et al*. 2007) and it is clear here (Fig. 11(b)) at large inclination angles the axial component of the pull out mechanism is not dominant and rupture tends to occur due to attainment of the ultimate strain capacity of the steel at the exit point of the matrix. Fig. 10 indicates that for fibres at inclination angle up to 15°, the values of the pull-out load are significantly increased with respect to the ones obtained for aligned fibres. On the other hand, for fibres at 30°, the corresponding load values are not greater than those obtained for fibres at 15° and in fact, they are slightly lower. Moreover, the pull-out strength of the fibre inclined by 45° is lower than that obtained for inclination angles of 15° and 30°. In any case, the pull-out load values of all the studied inclined fibres are greater than those of the aligned fibre. It is important to be mentioned here that these results agree with experiments of Banthia and Trottier (1994) and Robins *et al.* (2002), which indicate that the optimal fibre inclination angles may be within 10°-30° with increments at peak load with respect to aligned fibres up to 20%. In the cases studied here, fibres at 15° present a peak load 16% higher compared to the one obtained for aligned fibres, whereas the peak load for fibres at 30° is 12% higher compared to the corresponding load of aligned fibres.

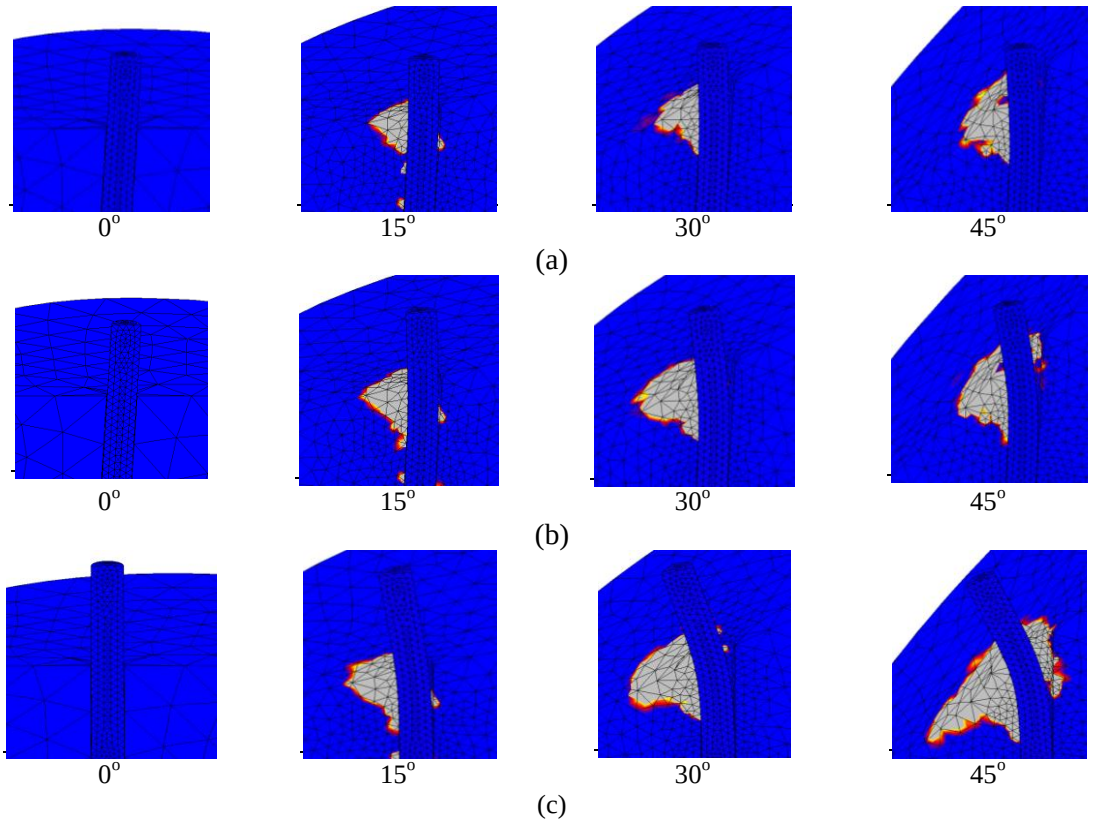


Fig. 13 Plastic strains in the matrix for a displacement (a) $\delta$=0.25 mm, (b) $\delta$=0.5 mm and (c) $\delta$=1.0 mm (the plastic strains in the grey area lie beyond the crushing strain limit)

The above described decrease of the pull-out load values at large inclination angles of the fibres is a result of another phenomenon that takes place during the pull-out of the inclined fibres; the crushing of the cementitious matrix near the exit point of the fibre. Figs. 13(a)-13(c) depict the evolution of plastic deformations of the matrix near the exit point of the fibre for strain values greater than 0.005, when the compressive strength of the matrix is almost zeroed and matrix crushing occurs. The figures represent actually the spalling that takes place in the matrix for all the studied cases for a displacement of 0.25 mm, 0.5 mm and 1.0 mm respectively. In the figures, the absence of plastic strains in the matrix near the exit point of the aligned fibre is observed. However, for all the cases of the inclined fibres, plastic strains that have exceeded the value of 0.005 occur in this area as it was expected. These cone-shaped volumes of the cementitious matrix actually represent the volume of the material that has lost its compressive strength and therefore, is inactive and unable to further resist the pull-out of the inclined fibre. It can be noticed that the size of the cone-shaped volumes becomes larger with the increase of the inclination angle of the fibre. Moreover, this size increases during the pull-out process and it is stabilized at higher values of displacements as the inclination angle increases (see diagrams of Fig. 13).

This fact can explain the lower pull-out load values of the fibres under significant inclination angles, as there is less resistance in this specific area to the pull-out from the matrix. The existence of these cones of inactive material may also explain the fact that, although the stiffness of the

model at $15^o$ is increased with respect to the stiffness of the model of the aligned fibre, the models with higher inclination angles (i.e. $30^o$ and $45^o$) exhibit slightly decreased stiffness (see diagrams of Fig. 10). These differences in the stiffness of the pull-out models begin to be more evident after a displacement of 0.1 mm, when the cones of crushed material begin to occupy a significant volume.

## 6. Conclusions

In this work a 3D numerical model to describe the pull-out response of inclined fibres with hooked ends was developed. The model is based on representative geometric and strength properties of constituent materials and on experimental data of fibres aligned with the load direction. This model was used for simulating the pull-out tests of an aligned fibre and of inclined fibres with inclination angles of $15^o$, $30^o$ and $45^o$. From the study it can be concluded that different inclination angles have as a result different maximum values of the pull-out load. More specifically, it was observed that:

- Fibres at $15^o$ present a peak load 16% higher compared to the one obtained for an aligned fibre. However, as the inclination angle further increases, the maximum value of the pull-out load slightly decreases, as it was observed for fibres at $30^o$ and $45^o$.
- The increase of the inclination angle has similar effects to the stiffness of the pull-out models, as well as to the pull-out load values. The stiffness of the model of the fibre at $15^o$ is increased with respect to the stiffness of the model of the aligned fibre, but for higher inclination angles the stiffness is decreased.
- The lower stiffness and peak load for higher inclination angles can be explained by the fact that crushing of the cementitious matrix occurs around the exit point of the fibres, as the plastic strains exceed the value of 0.005. The cone-shaped volumes that are formed there represent the inactive volume of material that can no further resist the pull-out of the fibre (Fig. 13). More specifically, the matrix spalling relieves bending stress at fiber exit points, leading to lower bound values for the ultimate tensile strength and lower stiffness of inclined fibres.
- Finally, it was observed that for fibres under large inclination angles the axial component of the pull-out mechanism is not dominant and rupture tends to occur due to attainment of the ultimate strain capacity of the steel at the exit point from the matrix **(**Fig. 11).

## References

Armelin, H. and Banthia, N. (1997), "Predicting the flexural postcracking performance of steel fibre reinforced concrete from the pull-out of single fibres", *ACI. Mater. J.*, **94**(1), 18-31.

Alwan, J.M., Naaman A.E. and Guerrero, P. (1999), "Effect of mechanical clamping on the pull-out response of hooked steel fibres embedded in cementitious matrices", *Concrete. Sci. Eng.*, **1**(1), 15-25.

Balaguru, P.N., Narahari, R. and Patel, M. (1992), "Flexural toughness of steel fibre reinforced concrete", *ACI. Mater. J.*, **89**(6), 541-546.

Banthia, N. and Trottier, J.F. (1994), "Concrete reinforced with deformed steel fibres, part I: bond-slip mechanisms", *ACI. Mater. J.*, **91**(5), 435-446.

Bartos, P.J.M. and Duris, M. (1994), "Inclined tensile strength of steel fibres in a cement-based composite", *Composites*, **25**(10), 945-952.

Chanvillard, G. and Aïtcin, P.C. (1996), "Pull-out behavior of corrugated steel fibres", *Adv. Cement. Based.*

*Mater.*, **4**(1), 28-41.
Cunha, V.M.C.F, Bartos, J.A.O. and Cruz, J.S. (2007), "Pull-out behavior of hooked-end steel fibres in self-compacting concrete", *Report 07-DC/E06*, Universidate do Minho.
Dupont, D. and Vanderwalle, L. (2005), "Distribution of steel fibres in rectangular sections", *Cement. Concrete. Comp.*, **27**(3), 391-398.
Ezeldin, S. and Lowe, S.R. (1991), "Mechanical properties of steel fibre reinforced rapid-set materials", *ACI. Mater. J.*, **88**(4), 384-389.
Georgiadi-Stefanidi, K., Mistakidis, E., Pantousa, D. and Zygomalas, M. (2010a), "Numerical modelling of the pull-out of hooked steel fibres from high-strength cementitious matrix, supplemented by experimental results", *Constr. Build. Mater.*, **24**(12), 2489-2506.
Georgiadi-Stefanidi, K., Mistakidis, E., Perdikaris, P. and Papatheocharis, T. (2010b), "Numerical simulation of tested reinforced concrete beams strengthened by thin fibre-reinforced cementitious matrix jackets", *Earthq. Struct.*, **1**(4), 345-370.
Kangaj, C.M., Inglis, H.M., Pietra, F. and Kok, S. (2014), "Numerical modelling of the pull-out of hooked-end steel fibre from epoxy matrix", *Proceedings of the 9th South African Conference on Computational and Applied Mechanics*, Somerset West, January.
Laranjeira, F., Aguado, A. and Molins, C. (2010a), "Predicting the pullout response of inclined straight steel fibres", *Mater. Struct.*, **43**(6), 875-895.
Laranjeira, F., Molins, C. and Aguado, A. (2010b), "Predicting the pullout response of inclined hooked steel fibres", *Cement. Concrete. Res.*, **40**(10), 1471-1487.
Lee, Y., Kang, S.T. and Kim, J.K. (2010), "Pullout behaviour of inclined steel fibre in an ultra-high strength cementitious matrix", *Constr. Build. Mater.*, **24**(10), 2030-2041.
Li, C.Y. and Mobasher, B. (1998), "Finite element simulations of fibre pull-out toughening in fibre reinforced cement based composites", *Adv. Cement. Based. Mater.*, **7**(3-4), 123-132.
Mobasher, B. and Li, C.Y. (1995), "Modelling of stiffness degradation of the interfacial zone during fibre debonding", *Compos. Eng.*, **5**(10-11), 1349-1365.
Pailleve, M., Buil, M. and Serrano, J.J. (1989), "Effect of fibre addition on the autogenous shrinkage of silica fume concrete", *ACI. Mater. J.*, **86**(2), 139-144.
Papanikolaou, V.K. and Kappos, A.J. (2007), "Confinement-sensitive plasticity constitutive model for concrete in triaxial compression", *Int. J. Solids. Struct.*, **44**(21), 7021-7048.
Pompo, A., Stupac, P.R., Nicolais, L. and Marchese, B. (1996), "Analysis of steel fibre pull-out from a cement matrix using video photography", *Cement. Concrete. Comp.*, **18**(1), 3-8.
Ramakrishnan, V., Wu, G.Y. and Hosalli, G. (1989), "Flexural behaviour and toughness of fibre reinforced concretes", Transportation Research Record, 1226, 69-77.
Robins, P., Austin, S. and Jones, P. (2002), "Pull-out behaviour of hooked steel fibres", *Mater. Struct.*, **35**(7), 434-442.
Shannag, M.J., Brincker, M. and Hansen, W. (1996), "Interfacial (fibre-matrix) properties of high-strength mortar (150 MPa) from fibre pull-out", *ACI. Mater. J.*, **93**(5), 1-7.
Soetens, T., Van Geysel, A., Matthys, S. and Taerme, L. (2013), "A semi-analytical model to predict the pull-out behavior of inclined hooked-end steel fibres", *Constr. Build. Mater.*, **43**, 253-265.
Sujivorakul, C., Waas, A.M. and Naaman, A.E. (2000), "Pull-out response of a smooth fiber with an end anchorage", *J. Eng. Mech. - ASCE.*, **126**(9), 986-993.
Tsai, J.H., Patra, A. and Wetherhold, R. (2005), "Finite element simulation of shaped ductile fibre pull-out using a mixed cohesive zone/friction interface model", *Compos. Part. A. - Appl. S.*, **36**(6), 827-838.
Zhan, Y. and Meschke, G. (2014), "Analytical model for the pull-out behaviour of straight and hooked-end steel fibres", *J. Eng. Mech. - ASCE.*, **140**(12).

*JK*